Scientia Iranica C (2012) 19 (3), 579–584

Sharif University of Technology

Scientia Iranica

Transactions C: Chemistry and Chemical Engineering

www.sciencedirect.com

Simulation of flow of short fiber suspensions through a planar contraction

M. Khodadadi Yazdi, A. Ramazani S.A. *, A. Kamyabi, H. Hosseini Amoli

Department of Chemical and Petroleum Engineering, Sharif University of Technology, Tehran, P.O. Box 11155-9313, Iran

Received 4 January 2011; revised 23 August 2011; accepted 13 December 2011

KEYWORDS

Short fiber;
Orientation;
Simulation;
Planar contraction;
Viscoelastic.

Abstract In this study, the flow of a fiber filled viscoelastic matrix through planar contractions is investigated. It was found that by adding fiber to the matrix vortex, the intensity increases. Fiber orientation along "*x*" and "*y*" axes was studied too. It was found that fiber orientation could be used for determining the flow regime through the contraction geometry. The rigidity condition of fibers, which needs the trace of the orientation tensor to be unity everywhere in the domain, is correct except near walls and the reentrant corner, which is slightly less than one. In these regions, the stress magnitude is higher, which results in more numerical errors, and which further leads to some error in predicting the orientation tensor. The first normal stress difference distribution along different axes was also studied in this article. It was found that increasing the volume concentration of fibers results in first normal stress difference intensification.

1. Introduction

Contraction flow has attracted many studies, since it has very important industrial applications, such as extrusion and molding polymer melts [1]. Furthermore, it can be used for measuring the flow properties of Non-Newtonian fluids, such as polymer melts and polymeric solutions, which exhibit highly non-Newtonian behavior [2] and whose properties lie between purely viscous Newtonian fluids and completely elastic solid [3]. Consequently, more complicated constitutive equations, including Giesekus, Oldroyd-B, Phan–Thien–Tanner (PTT), FENE-P etc. have been used for evaluating the extra stress tensor. The complex structure of the polymer chain leads to some amazing phenomena, including die swell or Barus effect, tubeless siphon, rod climbing and elastic recoil [1–3]. The flow pattern in contraction geometry is very complex. Near the walls, shear flow dominates, while at the centerline, a purely elongational flow occurs [4].

* Corresponding author.
E-mail address: Ramazani@sharif.edu (A. Ramazani S.A.).

Peer review under responsibility of Sharif University of Technology.

Production and hosting by Elsevier

Numerous studies have dealt with the contraction flow, both numerically and experimentally. In experimental investigations, some authors have used optical methods, such as Laser-Doppler Velocimetry (LDV), Flow Induced Birefringence (FIB) [5,6] and Digital Particle Image Velocimetry (DPIV) [7], in order to measure the velocity and stress fields.

There are many more numerical studies for both Newtonian [8] and non-Newtonian fluids [9–17]. For instance, Vrentas et al. [8] were the first to numerically study the creeping flow of a Newtonian fluid through an axisymmetric contraction.

In fiber suspensions, complex viscoelastic properties of a matrix, coupled with complexity, due to fiber–fiber, fiber-matrix and wall-fiber interactions, fiber re-orientation, fiber breakage and migration, result in very complicated rheological behavior for fiber-filled viscoelastic matrices. There are many numerical and experimental studies on the investigation and prediction of the rheological properties of fiber suspensions.

For a suspension of solid particles, the relative viscosity is mostly a function of the solid volume fraction, while for fiber suspensions, relative rheological functions are functions of the fiber volume fraction, the aspect ratio of fibers, fiber orientation and matrix properties [18]. It is worth mentioning that fiber diameter plays an important role in properties of fiber suspension, because during measurement of the rheological properties of suspension, fibers become aligned in the flow direction, such that the diameter would be the most important dimension of the fiber.

1026-3098
doi:10.1016/j.scient.2012.04.008

Table 1: Viscoelastic matrix parameter used in simulation.

ρ (kg/m^3)	η_s (kg/m.s)	η_p (kg/m.s)	λ (s)
1000	0.001	1.21	0.01

Flow characteristics of the suspension of the fiber in a thermoplastic media can be affected by the presence of fibers. On the other hand, when the molten polymer flows, fluctuating stresses modify fiber motion and orientation.

The first to study the flow of fiber suspension was Jeffery [19], followed by Batchelor [20], Cox and Brenner [21], and many more. However, most of these studies focus on dilute suspensions. Flow of a fiber suspension in contraction geometry has been studied by Lipscomb et al. [22] and Chiba and Nakamura [23]. Azaiez et al. [24] studied the flow of rigid fibers through a planar 4:1 contraction. They used three models, including PTT, FENE-CR and Carreau, for viscoelastic and Newtonian matrices. They found that fiber orientation is mostly affected by viscous effects. In places far enough from vortices, fiber orientation is not affected by matrix type, but near contraction walls, fibers are more orientated in polymer matrices. They also concluded that vortex intensity is reciprocally related to fiber orientation in the vortex region. An increase in fiber aspect ratio or concentration also results in a slightly more orientated state and a more intense vortex.

In this study, the flow dynamic and fiber orientation for flow of a fiber suspension in contraction geometry and fiber orientation are studied. A finite volume approach is used to solve constitutive equations of fiber suspensions in this geometry. The effect of numerical errors on predicting orientation tensor is investigated too.

2. Governing equations

In this study, the isothermal flow of a viscoelastic fluid containing fibers, through a planar contraction, is studied. Continuity and momentum equations for an incompressible viscoelastic matrix are as follows:

$$\nabla \cdot u = 0, \tag{1}$$

$$\frac{\partial(\rho u)}{\partial t} + \rho u \cdot \nabla u = -\nabla P + \nabla \cdot \tau^c, \tag{2}$$

where ρ denotes the fluid density, u is the velocity vector, p is pressure, and τ^c is the composite stress tensor. Lipscomb et al. [22] have proposed a constitutive equation for dilute particle suspension. For ellipsoids with a high aspect ratio, the equation can be written as follows [25]:

$$\tau^c = \eta_m \gamma + \eta_m \psi \{\mu_1 \gamma + \mu_2 \gamma : a_4\}, \tag{3}$$

where η_m is the matrix viscosity that is calculated from matrix constitutive equations which is Newtonian or generalized Newtonian or viscoelastic. In this study, a viscoelastic matrix was considered with parameters shown in Table 1, where η_s and η_p are solvent and polymer viscosity and λ denotes the relaxation time. In Eq. (3), ψ denotes fiber volume concentration, μ_1 and μ_2 are rheological coefficients, and γ is the stress rate expressed by:

$$\gamma = \nabla u + \nabla u^t, \tag{4}$$

in which superscript "t" denotes the transpose of the matrix. In Eq. (3), the last term is a representative of coupling between fiber orientation and hydrodynamic forces. The expression $\gamma : a_4$ is given by the quadratic closure approximation, given by:

$$\gamma : a_4 = tr(\gamma \cdot a)a, \tag{5}$$

in which "a_4" and "a" denote the fourth-order and second order orientation tensors, respectively, and "$tr()$" denotes the trace of the tensor. There are several relation for μ_1 and μ_2. For ellipsoids with large aspect ratio, this coefficient is given by Lipscomb et al. [22]:

$$\mu_1 = 2, \tag{6}$$

$$\mu_2 = \frac{r^2}{2\ln(r)}, \tag{7}$$

where "r" denotes the ellipsoids aspect ratio. Tensor "a" is the orientation tensor for non-dilute suspension, given by Folgar and Tucker [26]:

$$\frac{da}{dt} = -\frac{1}{2}(\omega \cdot a - a \cdot \omega) + \frac{1}{2}\xi(\dot{\gamma} \cdot a + a \cdot \dot{\gamma} - 2\dot{\gamma} : a_4) + 2C_I \bar{\dot{\gamma}}(\delta - ma), \tag{8}$$

in which, the last term describes the interaction between neighboring fibers. Parameter "m" is 2 and 3 for two and three dimensional geometries, respectively. Tensor δ is the identity tensor, γ is the shear rate tensor (Eq. (4)), and ω is the vorticity tensor given by:

$$\omega = \nabla u - \nabla u^t. \tag{9}$$

In Eq. (8), ξ is given by:

$$\xi = \frac{r^2 - 1}{r^2 + 1}, \tag{10}$$

where "r" is the ellipsoid aspect ratio:

$$r = \frac{L_f}{D_f}, \tag{11}$$

in which, L_f and D_f are length and diameter of the fibers, respectively. In Eq. (8), C_I is a phenomenological constant exhibiting fiber–fiber interactions. There are several relations for estimating C_I. In this paper, we used the following form:

$$C_I = 0.0184 \exp(-0.7148 \psi r). \tag{12}$$

In Eq. (12), "r" is the fiber aspect ratio, given by Eq. (11).

Finally, these relations were implemented in the OpenFOAM software package. This software is open source software in which the user can implement new solvers and/or transport models in the source codes. The software uses a finite volume approach for solving the PDE set.

3. Geometry and mesh

A planar geometry, shown in Figure 1, is used for numerical simulations. The length was considered long enough to reach a fully developed condition. A non-uniform mesh is used for numerical simulation, which is exhibited in Figure 2. There are 47 700 cells in the used mesh in the simulation.

4. Results and discussion

A suspension of 10% volume of fibers with aspect ratio of 20 was investigated. Figure 3 shows the a_{11}, which shows the

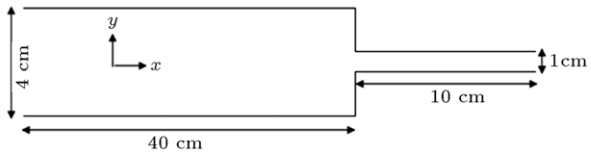

Figure 1: Geometry used for numerical simulation.

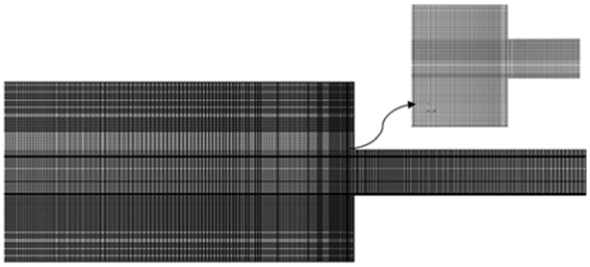

Figure 2: A non-uniform mesh used for numerical simulation.

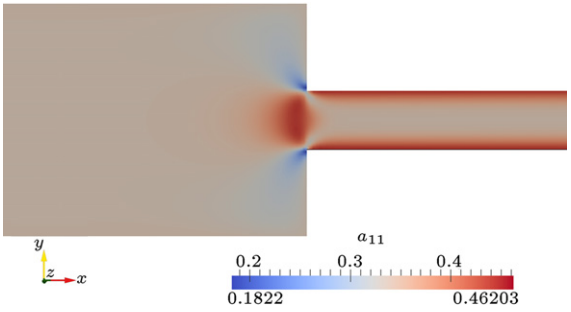

Figure 3: a_{11} in part of contraction geometry.

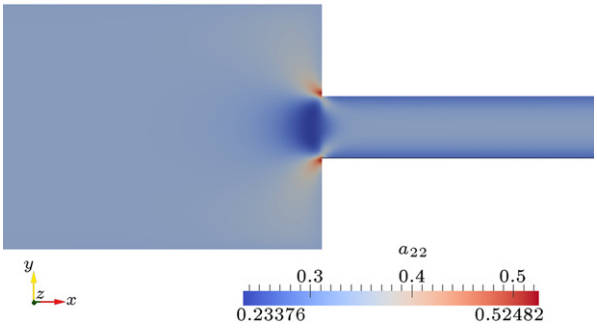

Figure 4: a_{22} in part of contraction geometry.

ellipsoid diameter along the x direction. It can clearly be seen that ellipsoids are more stretched near the die walls, because of shear stress exerting on fibers, and also just before the entrance region. In the entrance region, there is an elongational flow, which results in an enhancement in fiber orientation along the "x" axis (a_{11}). Next to the re-entrant corner, the a_{11} is small, because of fluid flow along the "y" direction in this section (elongation along "y").

Figure 4 shows a_{22}, which is the representative of the ellipsoid diameter along the "y" direction. As discussed before, for rigid fibers, the trace of tensor "a" should be unity. So, increasing a_{11} results in a decrement in a_{22} and vice versa, as shown in Figures 3 and 4.

Figure 5 exhibits that limitation "$trace\ (a) = 1$" is correct everywhere in the domain except at locations in which there

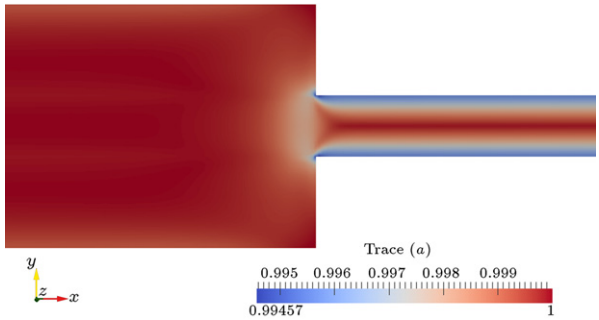

Figure 5: Trace of orientation tensor in the contraction geometry.

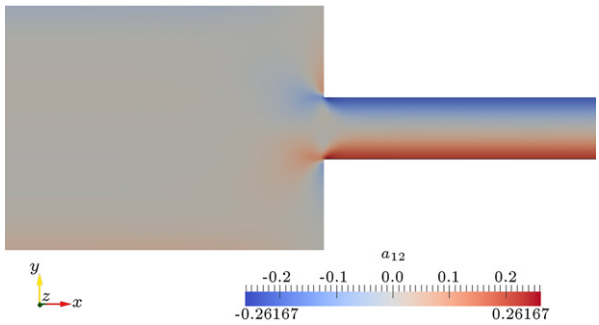

Figure 6: a_{12} in part of contraction geometry.

are intense stresses, such as at die walls in narrow sections. In these regions, numerical errors are bigger compared to inner sections, which leads to trace (a) not being exactly unity, but near one.

Figure 6 shows the a_{12} component of the orientation tensor, which describes the angle between fiber axes and the "x" direction. The symmetry in Figure 6 shows that fibers have an opposite orientation in the upper and lower sides of the symmetry plane. Positive values in the lower half denote that there is a positive angle between the fiber axis and the positive "x" direction. Moreover, negative values for a_{12} in the upper half show that the fiber axis makes a negative angle with the "x" direction.

For further discussion, it is needed to define two dimensionless lengths. X and Y are dimensionless lengths along x and y direction, respectively, and are given by:

$$X = \frac{(x - 0.4)}{0.01}, \tag{13}$$

$$Y = \frac{y}{0.01}. \tag{14}$$

The ellipsoid diameter along the "x" direction (a_{11}) at the centerline is plotted versus "X". Two different concentrations were considered. In places far from the entrance region, i.e. $X < -4$ or $X > 3$, $a_{11} = 0.33$, which means that the fiber has taken a spherical shape. Approaching the entrance region, a_{11} increases, which mean that fibers are aligned in an "x" direction. In more concentrated solutions, there are more intense stresses, which lead the fiber to be more stretched. Thus, for more concentrated solutions, a_{11} is bigger in the same location.

Figure 8 shows the ellipsoids diameter along the "y" direction. As mentioned earlier, a_{11} and a_{22} behave reversely, as can be observed from Figures 7 and 8.

Figure 9 exhibits the a_{12} profile along the centerline. Along the centerline, the value of a_{12} is very low, which means that

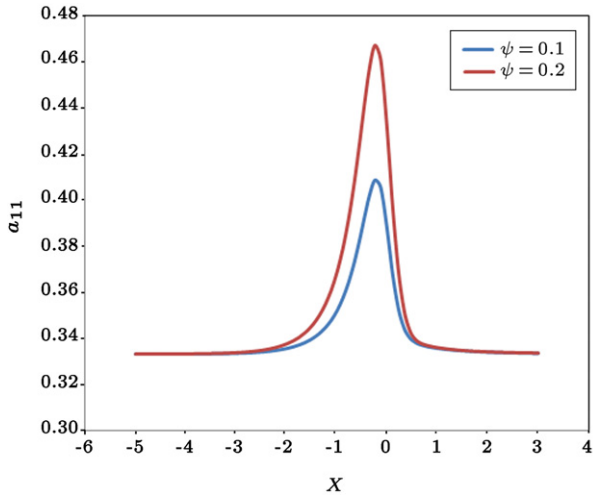

Figure 7: Ellipsoid diameter change along "x" direction at centerline for two suspensions with different volume concentrations.

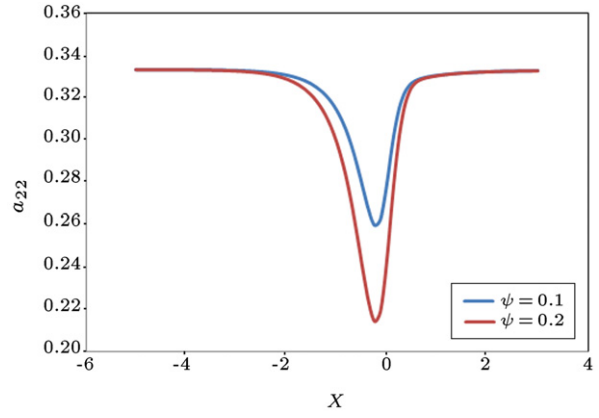

Figure 8: Ellipsoid diameter change along "y" direction, a_{22}, at centerline for two suspensions with different volume concentrations.

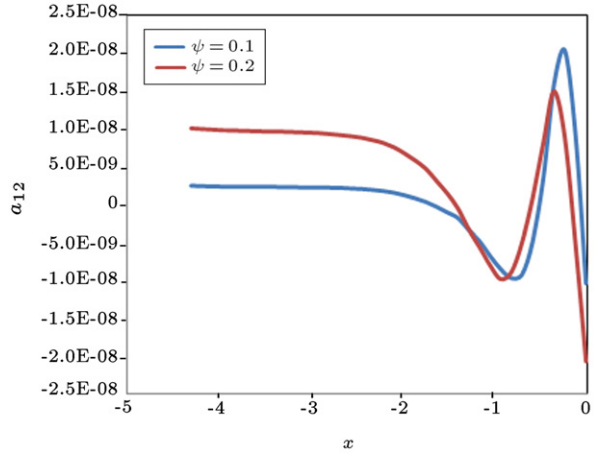

Figure 9: a_{12} change along "y" direction at centerline for two suspensions with different volume concentrations.

fibers are oriented along the "x" direction. There is a slight direction change just before the entrance ($X > -2$).

Figure 10 exhibits a_{11} for a suspension containing 10% fiber, along the "x" direction, at different distances from the

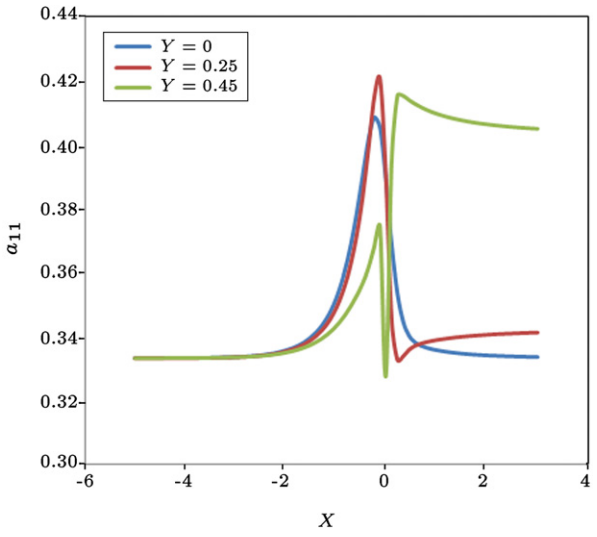

Figure 10: a_{11} for a suspension containing 10% fiber along "x" direction at different distances from the centerline.

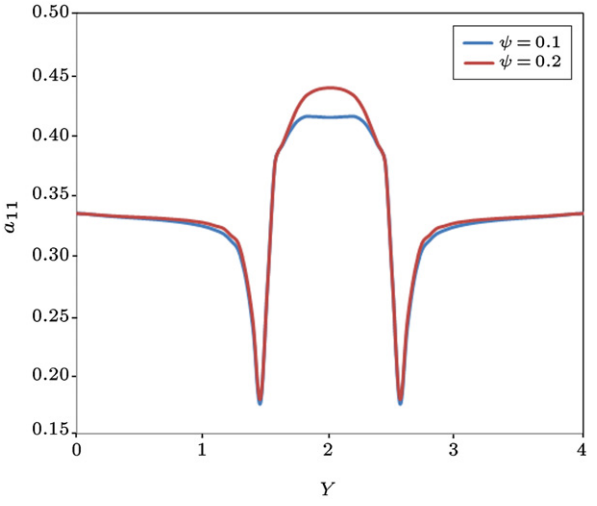

Figure 11: a_{11} at $X = -0.03$ along "y" direction.

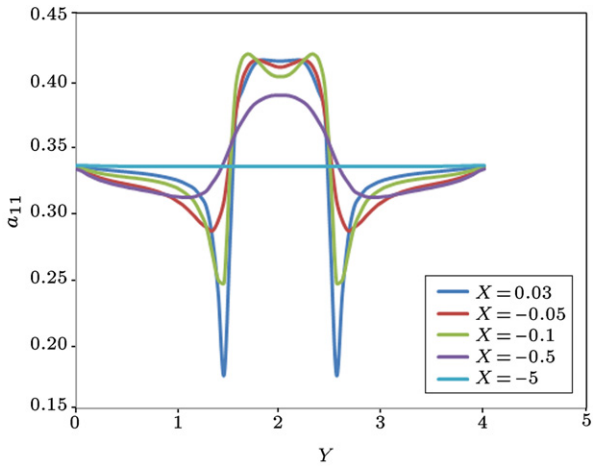

Figure 12: a_{11} at different distances from entrance along "y" direction.

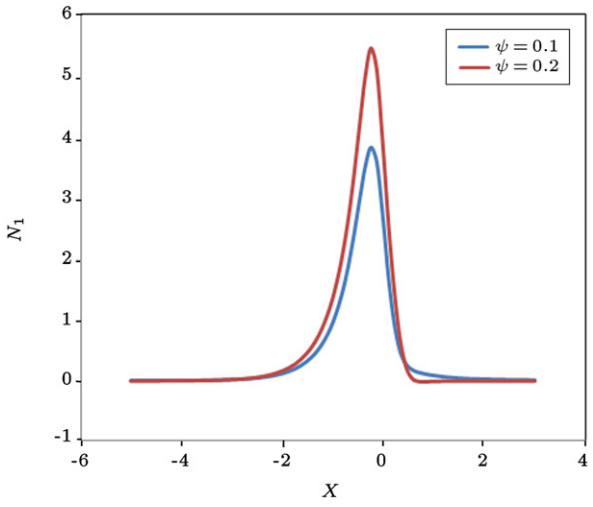

Figure 13: Normal stress distribution along centerline for $Y = 0$.

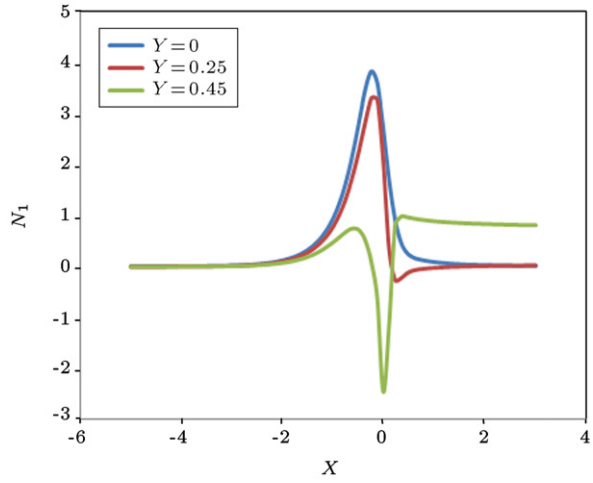

Figure 14: Normal stress distribution for different distances from centerline along "x" direction.

centerline. When "Y" tends to 0.5, such as $Y = 0.45$, there are two maximums and a minimum in the profile, while for smaller "Y", there is only a maximum. For $Y = 0$ and $Y = 0.25$, the maximum value for a_{11} shows the region near the entrance where elongational flow dominates. For $Y = 0.45$, the first maximum occurs approximately at the same X, followed by a minimum, which indicates the region of narrow die, where a side flow enters from the re-entrant corner, which is perpendicular to the main flow. Then the second maximum occurs in the narrow die, where there are more intense stresses near the die wall.

In other words, two maximum are related to just before entering the narrow die and at the die wall, and the minimum corresponds to a small region in the die that begins just after the re-entrant corner.

Figure 11 shows a_{11} along y direction for different concentrations in $X = -0.03$. The figure shows that there is a maximum at the center and two symmetric minimum near the re-entrant corner. There is a region in the center where aurceolate, like curvature, is observed, in which there is an intense elongational flow. But, next to this region, shear flow dominates, which leads to a linear increase in a_{11}.

Figure 12 shows a_{11} along y direction at different distances from the die entrance for a suspension of 10% volume of fiber in the matrix. At very distant locations, ellipsoids are at rest, and diagonal components are all 1/3, as shown for $X = 5$. Approaching the entrance, it is interesting that for places near the entrance region, some local recycling slight flow seems to occur, which leads to a minimum in the bell shaped section of the curve, as shown for $X = 0.1$ in Figure 12.

Figure 13 exhibits that the first normal stress difference is higher for suspension with a higher volume concentration of fibers.

Figure 14 exhibits a first normal stress difference along the x direction at different Y.

Figure 15 compares the vortex size for two suspensions of different fiber concentrations. As illustrated, vortex size increases with fiber concentration in the solution.

5. Conclusions

In this study, the flow of a viscoelastic matrix filled with different volume concentrations of rigid fibers in 4:1 planar contractions was investigated, using the OpenFOAM software package. The trace of tensor "a" should remain unity for rigid fibers, which was confirmed by calculating the trace of tensor "a" everywhere in the domain. It was found that vortex size increases with enhancing the volume concentration of fibers. For fiber motion along the "x" direction near the centerline, it was found that ellipsoid diameter along the "x" axis or a_{11} reaches a maximum just before entering the abrupt contraction, which corresponds to a minimum in a_{22} at the same point. However, if one considers fiber orientation along the x direction near the narrow section walls, two maximums and one minimum are observed, where the minimum occurs because of flow entering from the re-entrant corner in the "y" direction, which is perpendicular to the main flow direction, and causes a local traverse direction.

In the "y" direction near the entrance region, one maximum and two minimums are observed for a_{11} and the maximum is bigger for more concentrated suspensions. It was found that the fiber orientation can be used in determining flow type, i.e. where the shear flow or extensional flow dominates.

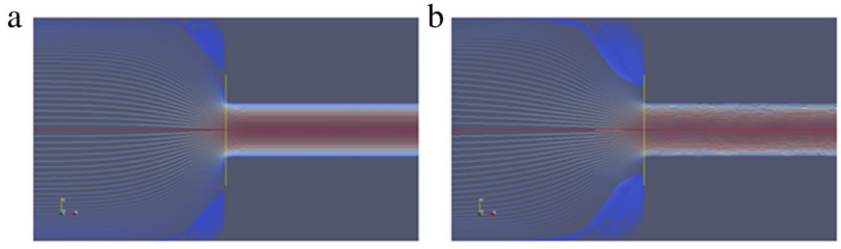

Figure 15: Vortex growth with increasing fiber volume concentrations. (a) $\psi = 0.01$; and (b) $\psi = 0.16$.

References

[1] Barnes, H., et al., *An Introduction to Rheology*, 1st Edn., Elsevier Ltd, London, UK, pp. 87–88 (1997).

[2] Bird, R., et al., *Dynamics of Polymeric Liquids*, 2nd Edn., vol. 1, pp. 21–22, John Wiley & Sons, New York, USA (1987).

[3] Makosco, C.W., *Rheology Principles Measurement and Applications*, Wiley-VCH, New York, USA, p. 8 (1994).

[4] Oliveira, M.S.N., et al. "Effect of contraction ratio upon viscoelastic flow in contractions: the axisymmetric case", *Journal of Non-Newtonian Fluid Mechanics*, 147, pp. 92–108 (2007).

[5] Quinzani, L.M., et al. "Birefringence and laser-doppler velocimetry (LDV) studies of viscoelastic flow through a planar contraction", *Journal of Non-Newtonian Fluid Mechanics*, 52, pp. 1–36 (1994).

[6] Martyn, M.T., et al. "Stress measurements for contraction flows of viscoelastic polymer melts", *Journal of Non-Newtonian Fluid Mechanics*, 91, pp. 123–142 (2000).

[7] Rothstein, J.P. and McKinley, G.H. "Extensional flow of a polystyrene Boger fluid through a 4:1:1 axisymmetric contraction/expansion", *Journal of Non-Newtonian Fluid Mechanics*, 86, pp. 61–88 (1999).

[8] Vrentas, J.S., et al. "Effect of axial diffusion of vorticity on flow development in circular conduits", *AIChE Journal*, 12, pp. 837–844 (1966).

[9] Mompean, G. "On predicting abrupt contraction flows with differential and algebraic viscoelastic models", *Computers & Fluids*, 31, pp. 935–956 (2002).

[10] Wachs, A. and Clermont, J. "Non-isothermal viscoelastic flow computations in an axisymmetric contraction at high Weissenberg numbers by a finite volume method", *Journal of Non-Newtonian Fluid Mechanics*, 95, pp. 147–184 (2000).

[11] Kim, J.M., et al. "High-resolution finite element simulation of 4:1 planar contraction flow of viscoelastic fluid", *Journal of Non-Newtonian Fluid Mechanics*, 129, pp. 23–37 (2005).

[12] Trebotich, D., et al. "A stable and convergent scheme for viscoelastic flow in contraction channels", *Journal of Computational Physics*, 205, pp. 315–342 (2005).

[13] Yesilata, B., et al. "Non-isothermal viscoelastic flow through an axisymmetric sudden contraction", *Journal of Non-Newtonian Fluid Mechanics*, 89, pp. 133–164 (2000).

[14] Xue, S.C., et al. "Three dimensional numerical simulations of viscoelastic flows through planar contractions", *Journal of Non-Newtonian Fluid Mechanics*, 74, pp. 195–245 (1998).

[15] Alves, M.A., et al. "On the effect of contraction ratio in viscoelastic flow through abrupt contractions", *Journal of Non-Newtonian Fluid Mechanics*, 122, pp. 117–130 (2004).

[16] Ganvir, V., et al. "Simulation of viscoelastic flows of polymer solutions in abrupt contractions using an arbitrary Lagrangian Eulerian (ALE) based finite element method", *Journal of Non-Newtonian Fluid Mechanics*, 143, pp. 157–169 (2007).

[17] Aguayo, J.P., et al. "The numerical prediction of planar viscoelastic contraction flows using the pom-pom model and higher-order finite volume schemes", *Journal of Computational Physics*, 220, pp. 586–611 (2007).

[18] Kitano, T. and Kataoka, T. "The rheology of suspensions of vinylon fibers in polymer liquids. II. Suspensions in polymer solutions", *RheolgicaActa*, 20, pp. 403–415 (1981).

[19] Jeffery, G.B. "The motion of ellipsoidal particles immersed in a viscous fluid", *Proceedings of The Royal Society of London. Series A*, 102, pp. 161–179 (1922).

[20] Batchelor, G.K. "The stress system in a suspension of force-free particles", *Journal of Fluid Mechanics*, 41(3), pp. 545–570 (1970).

[21] Cox, R.G. and Brenner, H. "The rheology of a suspension of particles in a Newtonian fluid", *Chemical Engineering Science*, 26, pp. 63–95 (1971).

[22] Lipscomb, G., et al. "The flow of fiber suspension in complex geometries", *Journal of Non-Newtonian Fluid Mechanics*, 26(3), pp. 297–325 (1988).

[23] Chiba, K. and Nakamura, K. "A numerical solution for the flow of dilute fiber suspensions through an axisymmetric contraction", *Journal of Non-Newtonian Fluid Mechanics*, 35(1), pp. 1–14 (1990).

[24] Azaiez, J., et al. "Investigation of the abrupt contraction flow of fiber suspensions in polymeric fluids", *Journal of Non-Newtonian Fluid Mechanics*, 73, pp. 289–316 (1997).

[25] Sepehr, M., et al. "Rheological properties of short fiber filled polypropylene in transient shear flow", *Journal of Non-Newtonian Fluid Mechanics*, 123, pp. 19–32 (2004).

[26] Folgar, F.P. and Tucker, C.L. "Orientation behavior of fibers in concentrated suspensions", *Journal of Reinforced Plastics and Composites*, 3, pp. 98–119 (1984).

Mohsen Khodadadi Yazdi received his B.S. degree from Ferdowsi University, Mashahd, Iran, and his M.S. degree from Sharif University of Technology, Tehran, Iran, in 2010. He is currently a Ph.D. degree student of Chemical Engineering at the Engineering Department of Tehran University. He has published more than 10 papers in international and national journals and at conferences. His research work includes: experimental and theoretical investigation of polymer processing and flow of polymeric and non-Newtonian fluids.

Ahmad Ramazani S.A received a Ph.D. degree from the Chemical Engineering Department of Laval University, Canada, in 1999, and since that time is a Professor of Chemical Engineering in the Department of Chemical and Petroleum Engineering at Sharif University of Technology, Tehran, Iran. He has published more than 200 papers in international and national journals and at conferences. He also published two text books on the subject of Heat Transfer and Rheology. His research works are in interdisciplinary subjects including: experimental and theoretical investigation of polymer relating processes and investigation of polymer properties and flow of polymeric and non-Newtonian fluids in different engineering fields, including biomedical and petroleum engineering related media.

During 2002–2003, he served as Head of the Biomedical Group and, during 2003–2008, as Head of the Polymer Engineering Group. He also was the executive chairman of the 8th International Seminar on Polymer Science and Technology held in 2007. He is guest editor of the Macromolecular Symposia Journal, Volume 274, published by Wiley-VCH, and was invited professor at the Ecole Polytechnique de Montreal in Canada in summer 2009, where he presented some of his research work as invited Professor in CREPEC.

Ata Kamyabi received his B.S. and M.S. degrees from the Department of Chemical Engineering at Sharif University of Technology, Tehran, Iran, where he is currently a Ph.D. degree candidate working on the numerical simulation of pore scale two-phase flow of viscoelastic materials using the Finite Volume Method (FVM).

Hadi Hosseini Amoli received a B.S. degree in Chemical Engineering from the Chemical and Petroleum Engineering Department at Sharif University of Technology, Tehran, Iran, in 2011.